Applied Physics A (2019) 125:717
https://doi.org/10.1007/s00339-019-3020-z

Applied Physics A
Materials Science & Processing

Investigation of the physical properties and gamma-ray shielding capability of borate glasses containing PbO, Al_2O_3 and Na_2O

M. S. Al-Buriahi[1] · Y. S. Rammah[2]

Received: 24 July 2019 / Accepted: 17 September 2019 / Published online: 21 September 2019

Abstract
Six glass samples of new lead borate with chemical formula $5Al_2O_3$–$5Na_2O$–(90-x)B_2O_3–xPbO, where $0 \le x \le 50$ mol% have been synthesized using the melt quenching technique. The prepared glasses distinguished by codes as $x = 0$ (ANBP00)—$x = 50$ (ANBP50) mol%. The physical properties and gamma-ray shielding capability of the glasses have been investigated. To achieve these aims, the amorphous structure of all glasses was examined using X-ray diffraction (XRD) measurements. The density and molar volume have been calculated. Density of the glasses increases from 2.133 (g/cm^3) for ANBP00 glass sample to 5.010 (g/cm^3) for ANBP50 sample. The XMuDat and XCOM programs were used to calculate the mass attenuation coefficient (μ/ρ) in the photon energy range of 0.015–10 MeV for all glasses. The difference between the obtained values of XMuDat and XCOM is found to be less than 1%. Half value layer (HVL), effective atomic number (Z_{eff}), and mean free path (MFP) as γ-ray shielding features have been evaluated using values of the (μ/ρ) for all proposed glasses. Results reveal that ANBP50 and ANBP00 samples possess a maximum Z_{eff} and a minimum Z_{eff}, respectively. Indeed, ANBP50 glass has lowest values of (HVL) and (MFP). Therefore, addition of PbO content in the prepared glasses has a considerable effect to improve the shielding effectiveness for these glasses. Finally, ANBP50 glass can be considered as a promising candidate for gamma-ray protection applications among different types of concretes, commercial glasses, and HMO glasses.

1 Introduction

Recently, heavy metal oxide (HMO) glasses have received more attenuation due to their structural advantages [1, 2]. These glasses can be used in several applications such as electronic and optical devices and solar energy [3, 4]. Borate glasses containing boron oxide (B_2O_3) are considered as promising amorphous materials with many advantages for their physical properties [5]. Adding small amounts of (BO_3) units into glass composition convert to (BO_4) units [6]. In addition, introducing lead oxide (PbO) into glass composition leads to enhanced density, linear and nonlinear optical properties [7]. It is well known that lead oxide in glass network can act dual role as network modifier at low PbO content and as glass former at high PbO content in the composition.

Radioactive isotopes are used in many different applications such as radiology, nuclear power and petroleum plants, agriculture, and industries. In addition, several kinds of radiation such as X/γ rays and neutrons can be produced from radioactive minerals and crushed rocks, nuclear power, nuclear reactors, chemical reactions, smoke detectors and others. While γ-photons have no mass and charge, it considered as one of the most energetic ionizing and dangerous radiations. Subsequently, it can travel for long distance and have high ability to pass through the materials.

Radiation exposure causes a lot of harmful effects in human health such as damage in genetic damage, blood cells, skin diseases, cancer and may be death. Thus, many researchers and investigators making good efforts to construct new radiation-shielding materials to reduce the harmful side effect of the radiation [8]. Materials used as radiation protection should possess homogeneity of chemical composition and density. To achieve this objective, glasses were prepared and examined for the protection against radiation by several authors [9–22]. From literature, the Pb is one of the most useful elements which can be chosen to add into glass composition to be good shielding materials. This is because, Pb is characterized by high density ($Z = 82$),

✉ Y. S. Rammah
dr_yasser1974@yahoo.com

[1] Department of Physics, Sakarya University, Sakarya, Turkey

[2] Department of Physics, Faculty of Science, Menoufia University, Shebin El-Koom 32511, Egypt

and this helps these materials to have high (μ/ρ) and small (HVL) and (MFP). Therefore, glasses containing Pb become more suitable and promise materials for radiation γ/X-ray and neutron-shielding properties [23].

In the present work, a group of six samples from lead borate glasses with chemical composition [$5Al_2O_3$–$5Na_2O$–$(90\text{-}x)B_2O_3$–xPbO: $0 \le x \le 50$ mol%] have been synthesized. The amorphous structure of these glasses was examined using X-ray diffraction (XRD) measurement technique. Density and molar volume of glasses were calculated. The radiation attenuation parameters of the prepared glasses were calculated using the XMuDat and XCOM programs to calculate the mass attenuation coefficient (μ/ρ) in the photon energy range of 0.015–10 MeV for glasses have been performed. A comparison between the obtained results of XMuDat and XCOM programs and the deviation ratio has been evaluated. (HVL), (Z_{eff}), and (MFP) as γ-ray shielding features have been evaluated using values of the (μ/ρ) for all proposed glasses.

2 Experimental and measurements

Reagent grades of Al_2O_3, Na_2CO_3, H_3BO_3, and PbO with high purity oxides (more than 99%) were used as starting materials to prepare a set of lead borate glasses with chemical composition $5Al_2O_3$–$5Na_2O$–$(90\text{-}x)B_2O_3$–xPbO, where $x = 0$, 10, 20, 30, 40, and 50 mol%. These glasses have been prepared using melt-quench technique. The produced glass samples were coded as $x = 0$ (ANBP00), $x = 10$ (ANBP10), $x = 20$ (ANBP20), $x = 30$ (ANBP30), $x = 40$ (ANBP0040), and $x = 50$ (ANBP50) mol%. For each sample composition, the powder form of the raw materials was weighted accurately, then mixed together using an agate mortar. The obtained mixture was melted in alumina crucibles at about 850–1000 °C for 35–4 min. The melting glasses stirred with an alumina rod to get glasses with good homogeneity. The result was a fluid with high viscous melts, poured into steel discs form. The produced glasses were annealed at 350–400 °C in another furnace for 1 h. Finally, annealing furnace was switched off and the glasses were left to cool gradually in situ for 24 h. Chemical compositions and weight fraction of elements in the prepared samples with their codes are listed in Table 1.

To detect the amorphous nature of the prepared glasses, powder X-ray diffraction (XRD) analysis using a Bruker, AXS D8 Advance, Germany ($Cu_{K\alpha}$ radiation) at room temperature was used.

To evaluate the density of the prepared glass samples, Automatic Gas Pycnometers for true density, Ultrapyc 1200e, and apparatus with helium gas was used.

3 Results and discussion

3.1 XRD measurements

The XRD patterns of the prepared glass samples (ANBP00–ANBP50) with a aforementioned formula from 10° to 80° is displayed in Fig. 1. Spectra in Fig. 1 show that all XRD measurements exhibit only humps around

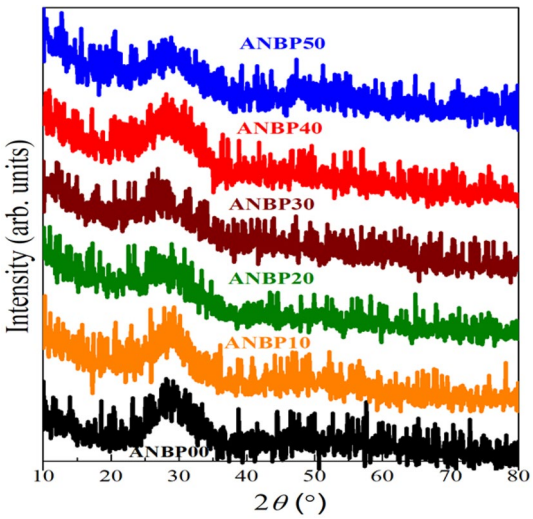

Fig. 1 XRD spectra for the prepared glasses (ANBP00–ANBP50)

Table 1 Chemical composition and weight fraction of elements in samples $5Al_2O_3$–$5Na_2O$–$(90\text{-}x)B_2O_3$–xPbO; $x = 0$, 10, 20, 30, 40, 50 mol% glasses

Sample code	Weight fraction mol%				Wt. fraction of elements in each sample					Density, ρ (g/cm^3)	Molar volume, V_m (cm^3/mol)
	B_2O_3	PbO	Al_2O_3	Na_2O	B	O	Na	Al	Pb		
ANBP00	90	0	5	5	0.279514	0.656931	0.037093	0.026463	0.000000	2.133	33.21847
ANBP10	80	10	5	5	0.248457	0.595156	0.037093	0.026463	0.092832	3.210	26.85763
ANBP20	70	20	5	5	0.217400	0.533381	0.037093	0.026463	0.185664	3.895	26.07368
ANBP30	60	30	5	5	0.186343	0.471607	0.037093	0.026463	0.278495	4.355	26.84661
ANBP40	50	40	5	5	0.155285	0.409832	0.037093	0.026463	0.371327	4.662	28.37559
ANBP50	40	50	5	5	0.124228	0.348057	0.037093	0.026463	0.464159	5.010	29.47006

$2\theta \sim 29°$ and have no sharp peaks. This affirms the amorphous nature of the prepared glasses.

3.2 Physical characterizations

The most suitable physical parameters tell us about the structure changes in the prepared glasses, density (ρ) and molar volume (V_m). The (ρ) and (V_m) mainly depend on compactness of structure of the samples. From the densities of the studied glasses, the corresponding molar volume has been calculated as:

$$V_m = \frac{M_w}{\rho}, \tag{1}$$

where M_w denotes the molecular weight and ρ is the density of the prepared glass sample. Densities and molar volumes for all prepared glasses are listed in Table 1. Dependence of density and molar volume of the glasses as a function of PbO concentration in mol% has been portrayed in Fig. 2. It is clear in Fig. 2 that the density increased from 2.123 to 5.010 g/cm^3 with increase in the PbO content from 0 to 50 mol%. This increase might be related to the high molecular weight of PbO (223.20 g/mol) than that of the replaced B_2O_3 (69.60 g/mol) concentration. Also, Fig. 2 displays the molar volume of the investigated glasses falls down to 20 mol% of PbO then raises linearly with increasing PbO concentration. This result confirms the behavior of dual role for PbO when it introduces into the glass network structure. The PbO acts as network modifier, while at high concentrations, PbO acts as network glass former and this leads to the conversion of B–O–B borate ring to continuous B–O–Pb lead borate series and the structure becomes more open [24].

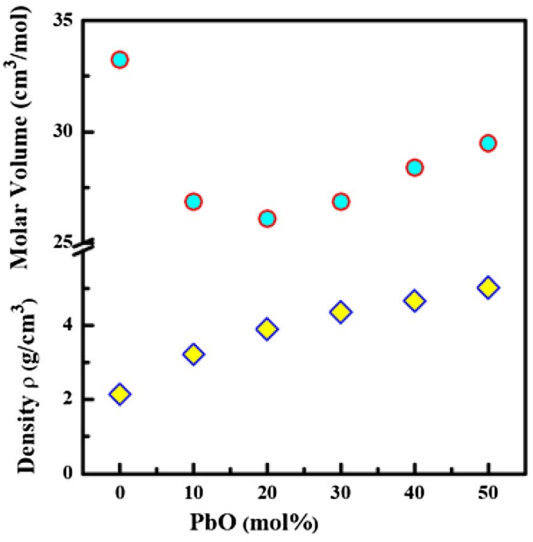

Fig. 2 Dependence of density (ρ) and molar volume (V_m) on PbO concentration in mol% in investigated glasses

3.3 Gamma-ray shielding features

Glass code, chemical composition, atomic composition and density of the prepared glasses are listed in Table 1. From Table 1, it is easily seen that the densities of the prepared glasses vary from a lower value (2.133 g/cm^3 for ANBP00 glass) to a higher value (5.010 g/cm^3 for ANBP50), due to the increment of PbO content from 0 to 50 mol%, respectively. The mass attenuation coefficient (μ/ρ) values for these glasses were calculated using XMuDat [25] and XCOM [26, 27] programs in the photon energy range of 0.015–10 MeV using [28]:

$$\frac{\mu}{\rho} = \sum_i W_i \left(\frac{\mu}{\rho}\right)_i \tag{2}$$

where w_i refers to the fractional atomic mass of the elements and $(\mu/\rho)_i$ is the mass attenuation coefficient for the individual elements in the sample.

The calculated values of (μ/ρ) with the deviation between XMuDat and XCOM for the six prepared glasses are listed in Tables 2 and 3. The deviation between XMuDat and XCOM values can be evaluated according to the following equation:

$$\text{Dev.} = \left| \left[\left(\frac{\mu}{\rho}\right)_{\text{XCOM}} - \left(\frac{\mu}{\rho}\right)_{\text{XMuDat}} \right] \div \left(\frac{\mu}{\rho}\right)_{\text{XCOM}} \right| \times 100. \tag{3}$$

From Tables 2 and 3, the estimated deviations (Dev.) in the prepared glass samples vary from 1.14 to 0.93% for ANBP00 glass, from 1.13 to 0.91% for ANBP10 glass, from 0.04 to 0.88% for ANBP20 glass, from 1.11 to 0.91% for ANBP30 glass, from 1.13 to 0.91% for ANBP40 glass and from 1.13 to 0.95% for ANBP50 glass. The obtained results reveal that the difference between the calculated values of XMuDat and XCOM is less than 1% and this confirms the accuracy of the present results.

From Tables 2 and 3, it is also noted that the (μ/ρ) values of the prepared glasses vary from the high values in the low-energy region to the low values in the high-energy region. This is attributed to the main photon interactions such that photoelectric interaction dominates in the low-energy regions. Compton scattering dominates in the intermediate-energy regions and the pair production is the dominating process in the high-energy region ($3 < E < 10$).

Figure 3 shows the effect of addition of PbO on gamma attenuation properties of the prepared glasses. It is seen clearly that the (μ/ρ) values have strong dependence of PbO content in low-energy region, weak dependence of PbO in intermediate-energy region and reasonable dependence of PbO in the high-energy region. The reason is that

Table 2 The mass attenuation coefficient (μ/ρ) values using XCOM and XmuDat and deviation between XMuDat and XCOM for glasses (ANBP00–ANBP20)

Energy (MeV)	ANBP00			ANBP10			ANBP20		
	XCOM	XmuDat	Dev.%	XCOM	XmuDat	Dev.%	XCOM	XmuDat	Dev.%
0.015	1.726	1.7421	0.93	11.95	11.854	0.8	22.18	22.355	0.79
0.02	0.8201	0.8241	0.49	8.776	8.756	0.23	16.73	16.626	0.62
0.03	0.3625	0.3636	0.3	3.147	3.1354	0.37	5.932	5.8895	0.72
0.04	0.2497	0.2491	0.24	1.561	1.5542	0.44	2.873	2.8654	0.26
0.05	0.2068	0.2057	0.53	0.9349	0.9311	0.41	1.663	1.6512	0.71
0.06	0.1853	0.1867	0.76	0.6346	0.6398	0.82	1.084	1.0863	0.21
0.08	0.1634	0.1645	0.67	0.3731	0.3765	0.91	0.5827	0.5839	0.21
0.1	0.1512	0.1512	0.26	0.6524	0.6552	0.43	1.154	1.1632	0.8
0.2	0.1207	0.1218	0.91	0.2022	0.2036	0.69	0.2838	0.2822	0.56
0.3	0.1044	0.1054	0.96	0.1322	0.1319	0.23	0.1599	0.1585	0.88
0.4	0.0934	0.0939	0.54	0.1063	0.1071	0.75	0.1192	0.1187	0.42
0.5	0.0852	0.0854	0.15	0.0923	0.0926	0.27	0.0994	0.1	0.57
0.6	0.0788	0.0784	0.51	0.0831	0.0836	0.65	0.0874	0.0877	0.38
0.8	0.0692	0.0693	0.19	0.071	0.0717	0.9	0.0728	0.0727	0.25
1	0.0622	0.0623	0.18	0.063	0.0631	0.13	0.0639	0.0637	0.28
2	0.0435	0.0437	0.39	0.0438	0.0437	0.09	0.044	0.0439	0.2
3	0.035	0.035	0.26	0.0357	0.0358	0.2	0.0364	0.0365	0.14
4	0.0301	0.0303	0.53	0.0313	0.0313	0.22	0.0324	0.0323	0.12
5	0.0269	0.0268	0.37	0.0284	0.0282	0.7	0.0299	0.0298	0.33
6	0.0247	0.0246	0.4	0.0265	0.0264	0.34	0.0283	0.0283	0.04
7	0.0231	0.0232	0.43	0.0252	0.0253	0.68	0.0272	0.0273	0.22
8	0.0218	0.0217	0.46	0.0242	0.0243	0.41	0.0265	0.0264	0.23
9	0.0208	0.0209	0.14	0.0234	0.0232	0.85	0.026	0.0259	0.19
10	0.0201	0.0201	0.35	0.0228	0.0229	0.13	0.0256	0.0257	0.20

in low-energy region the photoelectric process dominates and varies with $1/E^3$, in the intermediate-energy region the dominating process is Compton scattering which varies with $1/E$ and in the high-energy region the pair production is the dominating process and varies with log E. Therefore, it can be concluded that the glass sample containing 50 mol% of PbO (ANBP50) can be developed to be an excellent shielding material in gamma-ray application over the considered energy range.

To investigate the ability of the prepared glasses to serve in gamma shielding applications, we also calculated the Z_{eff} for the prepared glasses which represents the fraction of total number of electrons in the sample engaged in photon–atom interaction and can be calculated as [29, 30]:

$$Z_{\text{eff}} = \frac{\sum f_i A_i \left(\frac{\mu}{\rho}\right)_i}{\sum \frac{A_j}{Z_j} \left(\frac{\mu}{\rho}\right)_j}, \tag{4}$$

where Z_i and A_i denote the atomic number and atomic weight of the element i, respectively. The f_i refers to the fractional abundance of the ith element with respect to the number of atoms.

Figure 4 shows the calculated values of Z_{eff} for the prepared glasses and their variation with incident photon energies in the range 0.015–10 MeV. It is clear that the Z_{eff} values of the present glasses are found in the range of 7–79. It is also observed that ANBP50 glass possesses a maximum Z_{eff}, whereas ANBP00 possesses a minimum Z_{eff}. This is because the partial photon processes are directly related to Z (atomic number) of the material constituent elements. Such that the photoelectric process depends on Z^4 and the Compton process depends on Z. Therefore, the max. Z_{eff} is for ANBP50 glass which contains the highest weight fraction of Pb (0.464159%). And the min. Z_{eff} is for ANBP00 glass which is Pb-free. In the fact, the good shielding materials should have a higher Z_{eff}. For example, the gamma ray interacts more with high Z_{eff} materials leading to decrease the photon energy that becomes incapable to penetrate the material. Thus, ANBP50 is a better shielding material among the prepared glasses.

Half value layer (HVL) indicates shielding competence of the selected glasses against gamma ray (e.g., the lower HVL, the higher shielding competence). HVL values were calculated by Eq. (5) and drawn in Fig. 5.

$$\text{HVL} = \frac{0.693}{\mu}, \tag{5}$$

Table 3 The mass attenuation coefficient (μ/ρ) values using XCOM and XmuDat and deviation between XMuDat and XCOM for glasses (ANBP30–ANBP50)

Energy (MeV)	ANBP30			ANBP40			ANBP50		
	XCOM	XmuDat	Dev.%	XCOM	XmuDat	Dev.%	XCOM	XmuDat	Dev.%
0.015	32.41	32.651	0.74	42.64	42.32	0.75	52.87	52.937	0.13
0.02	24.69	24.721	0.13	32.64	32.357	0.87	40.6	40.457	0.35
0.03	8.716	8.6988	0.2	11.5	11.398	0.89	14.29	14.423	0.93
0.04	4.184	4.1757	0.2	5.496	5.4598	0.66	6.807	6.7856	0.31
0.05	2.391	2.379	0.5	3.119	3.112	0.22	3.848	3.8654	0.45
0.06	1.533	1.5435	0.68	1.982	1.9732	0.44	2.432	2.445	0.53
0.08	0.7924	0.7965	0.52	1.002	1.0094	0.74	1.212	1.2135	0.12
0.1	1.655	1.6512	0.23	2.156	2.1455	0.49	2.657	2.6554	0.06
0.2	0.3653	0.3676	0.63	0.4468	0.4454	0.31	0.5284	0.5252	0.61
0.3	0.1877	0.186	0.91	0.2155	0.2136	0.88	0.2432	0.2455	0.95
0.4	0.1321	0.1329	0.61	0.145	0.1461	0.76	0.1579	0.1565	0.89
0.5	0.1065	0.1059	0.56	0.1136	0.1138	0.18	0.1206	0.1215	0.75
0.6	0.0916	0.0918	0.13	0.0959	0.0959	0.07	0.1002	0.101	0.8
0.8	0.0747	0.0746	0.13	0.0765	0.0761	0.47	0.0783	0.0777	0.77
1	0.0647	0.0646	0.17	0.0655	0.0654	0.24	0.0664	0.0667	0.45
2	0.0443	0.0445	0.45	0.0445	0.0447	0.38	0.0447	0.0446	0.42
3	0.0371	0.0369	0.54	0.0378	0.0377	0.37	0.0385	0.0383	0.6
4	0.0335	0.0336	0.45	0.0346	0.0349	0.84	0.0357	0.0356	0.28
5	0.0314	0.0313	0.19	0.0329	0.0326	0.91	0.0343	0.0343	0.17
6	0.0301	0.0303	0.7	0.0319	0.032	0.22	0.0337	0.0337	0.18
7	0.0293	0.0291	0.65	0.0314	0.0316	0.64	0.0335	0.0338	0.81
8	0.0288	0.0286	0.9	0.0312	0.0311	0.13	0.0335	0.0338	0.9
9	0.0285	0.0283	0.77	0.0311	0.0313	0.64	0.0337	0.0338	0.24
10	0.0284	0.0284	0.11	0.0312	0.0313	0.26	0.034	0.0336	0.91

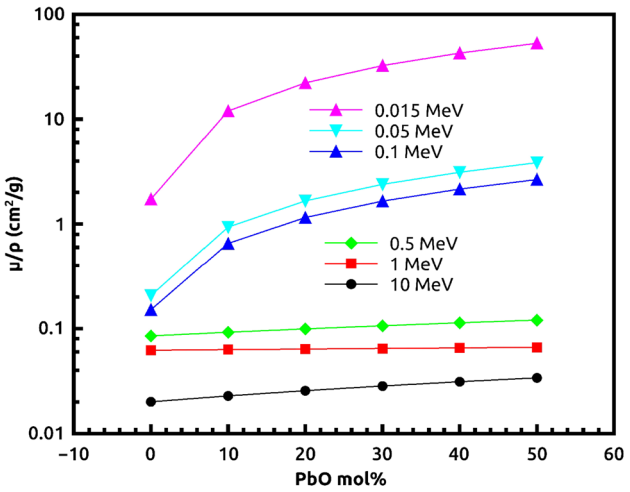

Fig. 3 Variation of the (μ/ρ) with PbO content for the investigated glasses at photon energies 0.015, 0.05, 0.10, 0.5, 1, and 10 MeV

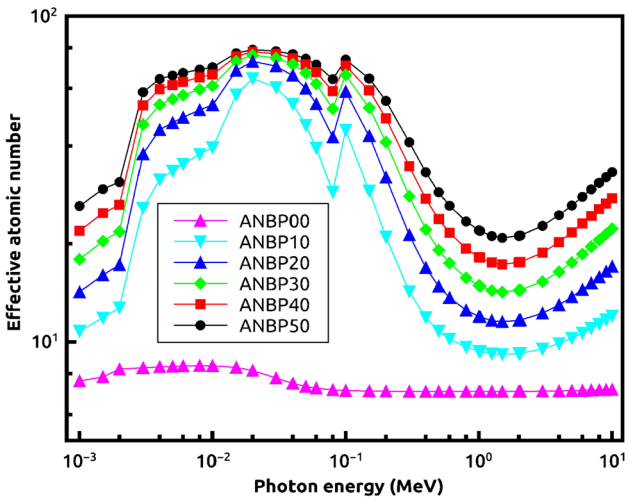

Fig. 4 The Z_{eff} for the investigated glasses (ANBP00–ANBP50)

where (μ) is the linear attenuation coefficient for each glass sample, which is the mass attenuation coefficient of the sample divide to its density. It is found that the HVL increases with increase in the incident photon energy, such behavior of HVL with incident photon energy can be explained similar to the aforementioned discussion of (μ/ρ) values. Moreover, it can be noted that the surplus of PbO content in the prepared glasses has a considerable effect to improve the shielding effectiveness for these glasses. Therefore, ANBP50 glass sample is a promising candidate for gamma-ray protection

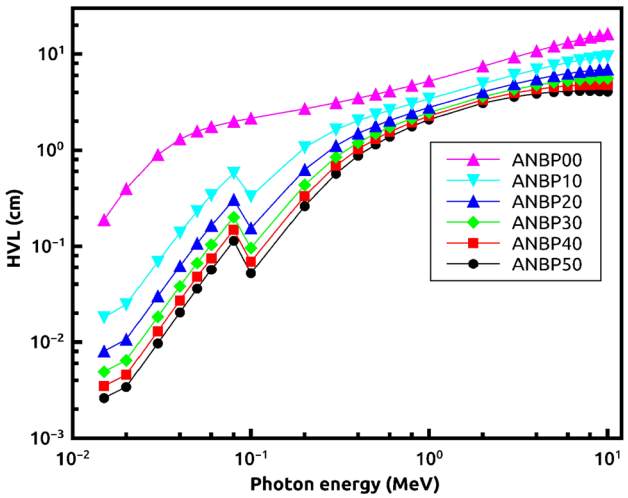

Fig. 5 The HVL for the investigated glasses (ANBP00–ANBP50)

applications among the prepared glass samples. In Fig. 6, ANBP50 glass is compared with ordinary concrete [31], marble concrete [32], and different commercial glasses such as RS-520, RS-360, and RS-253-G18 [33]. From this comparison, we found that our prepared ANBP50 glass possesses HVL values lower than those of ordinary concrete, marble concrete and commercial glass of RS-253-G18. Moreover, the values of HVL for ANBP50 are very close to those of commercial glasses in forms RS-520 and RS-360. Consequently, ANBP50 offers a superior gamma-ray shielding properties.

The average distance travelled by photon before its interaction again is measured by MFP which is $1/\mu$ in cm. The evaluation of MFP confirms the competence of the glasses under study as a promising radiation-shielding candidate.

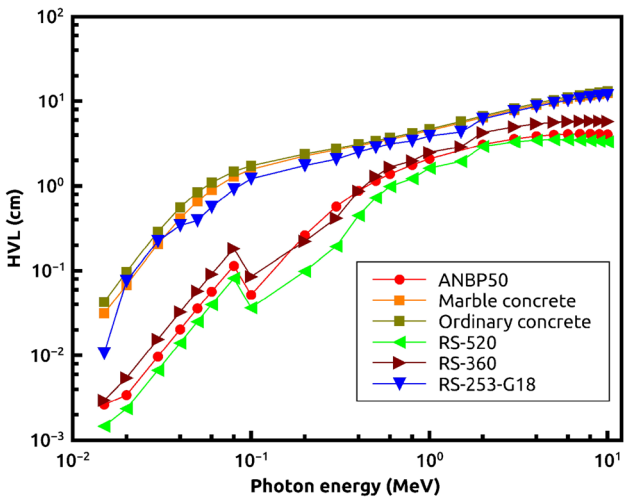

Fig. 6 Comparison between HVL of ANBP50 glass sample and some concretes and commercial glasses

Figure 7 represents the results of MFP for the prepared glasses as compared with newly published Pb-based glasses and other HMO glasses [34]. It is clear that the MFP is a small when the photon energy is low and becomes higher when the photon energy increases. Thus, in practical application it is better to increment the thickness of the glass because of the photons that are able to penetrate the glass more deeply. Furthermore, Fig. 7 shows economical sides for using the prepared glasses as gamma-ray-shielding material. Such that the MFP values of the prepared glasses were observed to be comparable with each of ZBPC75 [35], TVTi2 [36], TWEP [37], Te5 and Ge5 [12] glasses.

4 Conclusion

A group contains of six samples from lead borate glasses with chemical formula $5Al_2O_3$–$5Na_2O$–$(90\text{-}x)B_2O_3$–xPbO, where $x = 0$, 10, 20, 30, 40, and 50 mol% have been synthesized using the melt-quenching technique. The prepared glasses distinguished by codes as $x = 0$ (ANBP00), $x = 10$ (ANBP10), $x = 20$ (ANBP20), $x = 30$ (ANBP30), $x = 40$ (ANBP0040), and $x = 50$ (ANBP50) mol%. The physical properties and gamma-ray shielding capability of the glasses have been investigated. To achieve these aims, the X-ray diffraction (XRD) measurements confirmed that all prepared glasses are in amorphous structure. The density of the glasses is increased with increasing PbO content, and it was varied between 2.133 (g/cm^3) for glass sample ANBP00 and 5.010 (g/cm^3) for ANBP50 glass sample. The dual role of PbO behavior in the studied glass network is proved by the behavior of molar volume of the glasses. The XMuDat and XCOM programs were used to calculate the mass attenuation coefficient (μ/ρ) in the photon energy range

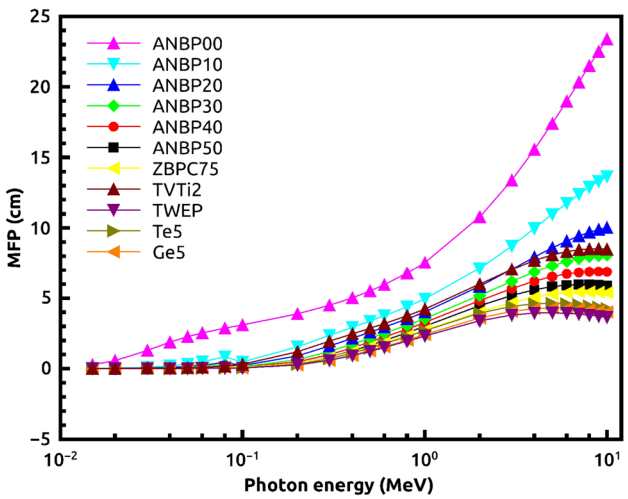

Fig. 7 The MFP of the investigated glasses (ANBP00–ANBP50) compared with that of some earlier published glasses

of 0.015–10 MeV for all glasses. The difference between the calculated values of XMuDat and XCOM is less than 1%. The (μ/ρ) values have strong dependence of PbO concentration in low-energy range, weak dependence of PbO in intermediate-energy region and reasonable dependence of PbO in the high-energy range. ANBP50 ($x = 50$ mol% of PbO) glass sample possesses a maximum Z_{eff}, whereas ANBP00 possesses a minimum Z_{eff}. Indeed, ANBP50 glass has lowest values of half value layer (HVL) and mean free path (MFP). Therefore, addition of PbO content in the investigated glasses has a considerable effect to improve the shielding effectiveness for these glasses. Thus, ANBP50 glass sample is a promising candidate for gamma-ray protection applications among the prepared glass samples.

Finally, it is concluded that the ANBP50 glass among the prepared glasses can be considered as a promising candidate for gamma/X-ray applications as compared with the ordinary concrete, marble concrete, and commercial glasses such as RS-360 and RS-253-G18.

Acknowledgements The authors would like to express his deep thanks appreciation to Prof. B. T. Tonguc, vice rector of Sakarya University, Turkey and Prof. R. El-Mallawany, Physics Department, Faculty of Science, Menoufia University, Egypt for their great support providing and all facilities necessary during this work.

References

1. E.I. Kamitsos, M.A. Kasakassides, Effect of melt temperature on glass structure. Phys. Chem. Glasses **30**, 235 (1989)
2. S.G. Motke, S.P. Yawale, S.S. Yawale, Infrared spectra of zinc doped lead borate glasses. Bull. Mater. Sci. **25**, 75–78 (2002)
3. V. Rajendaran, N. Palanivelu, H.A. El-Batal, F.A. Khalifa, N.A. Shafi, Effect of Al_2O_3 addition on the acoustical properties of lithium borate glasses. Acoust. Lett. **23**, 113–121 (1999)
4. H. Hirashima, D. Arari, T. Yoshida, Electrical conductivity of $PbO–P_2O_5–V_2O_5$ glasses. J. Am. Ceram. Soc. **68**, 486 (1985)
5. A. Terczynska-Madej, K. Cholewa-Kowalska, M. Łączka, Coordination and valence state of transition metal ions in alkali-borate glasses. Opt. Mater. **33**(12), 1984–1988 (2011)
6. H. Doweidar, Consideration of the boron oxide anomaly. J. Mater. Sci. **25**(1), 253–258 (1990)
7. R.S. Kaundal, S. Kaur, N. Singh, K.J. Singh, Investigation of structural properties of lead strontium borate glasses for gamma-ray shielding applications. J. Phys. Chem. Solids **71**(9), 1191–1195 (2010)
8. Ashok Kumar, Gamma ray shielding properties of $PbO–Li_2O–B_2O_3$ glasses. Radiat. Phys. Chem. **136**, 50–53 (2017)
9. D.K. Gaikwad, S.S. Obaid, M.I. Sayyed, R.R. Bhosale, V.V. Awasarmol, A. Kumar, M.D. Shirsat, P.P. Pawar, Comparative study of gamma ray shielding competence of $WO_3–TeO_2–PbO$ glass system to different glasses and concretes. Mater. Chem. Phys. **213**, 508–517 (2018)
10. A. Saeed, R.M. El Shazly, Y.H. Elbashar, A.M. Abou El-azm, M.M. El-Okr, M.N.H. Comsan, A.M. Osman, A.M. Abdalmonem, A.R. El-Sersy, Gamma ray attenuation in a developed borate glassy system. Radiat. Phys. Chem. **102**, 167–170 (2014)
11. K.J. Singh, S. Kaur, R.S. Kaundal, Comparative study of gamma ray shielding and some properties of $PbO–SiO_2–Al_2O_3$ and $Bi_2O_3–SiO_2–Al_2O_3$ glass systems. Radiat. Phys. Chem. **96**, 153–157 (2014)
12. R. El-Mallawany, M.I. Sayyed, M.G. Dong, Y.S. Rammah, Simulation of radiation shielding properties of glasses contain PbO. Radiat. Phys. Chem. **151**, 239–252 (2018)
13. M.I. Sayyed, Investigations of gamma ray and fast neutron shielding properties of tellurite glasses with different oxide compositions. Can. J. Phys. **94**, 1133–1137 (2016)
14. N. Singh, K.J. Singh, K. Singh, H. Singh, Comparative study of lead borate and bismuth lead borate glass systems as gamma-radiation shielding materials. Nucl. Instrum. Methods Phys. Res. B **225**, 305–309 (2004)
15. M.I. Sayyed, G. Lakshminarayana, I.V. Kityk, M.A. Mahdi, Evaluation of shielding parameters for heavy metal fluoride based tellurite-rich glasses for gamma ray shielding applications. Radiat. Phys. Chem. **139**, 33–39 (2017)
16. G. Lakshminarayana, S.O. Baki, M.I. Sayyed, M.G. Dong, A. Lira, A.S.M. Noor, I.V. Kityk, M.A. Mahdi, Vibrational, thermal features, and photon attenuation coefficients evaluation for $TeO_2–B_2O_3–BaO–ZnO–Na_2O–Er_2O_3–Pr_6O_{11}$ glasses as gamma rays shielding materials. J. Non Cryst. Solids **481**, 568–578 (2018)
17. M.I. Sayyed, G. Lakshminarayana, M.G. Dong, M.Ç. Ersundu, A.E. Ersundu, I.V. Kityk, Investigation on gamma and neutron radiation shielding parameters for $BaO/SrO–Bi_2O_3–B_2O_3$ glasses. Radiat. Phys. Chem. **145**, 26–33 (2018)
18. Y.S. Rammah, M.I. Sayyed, A.S. Abohaswa, H.O. Tekin, FTIR, electronic polarizability and shielding parameters of B_2O_3 glasses doped with SnO_2. Appl. Phys. A **124**, 650 (2018)
19. Y.S. Rammah, M.I. Sayyed, A.A. Ali, H.O. Tekin, R. El-Mallawany, Optical properties and gamma-shielding features of bismuth borate glasses. Appl. Phys. A **124**, 832 (2018)
20. Y.S. Rammah, A. Askin, A.S. Abouhaswa, F.I. El-Agawany, M.I. Sayyed, Synthesis, physical, structural and shielding properties of newly developed $B_2O_3–ZnO–PbO–Fe_2O_3$ glasses using Geant4 code and WinXCOM program. Appl. Phys. A **125**, 523 (2019)
21. M.I. Sayyed, I.A. El-Mesady, A.S. Abouhaswa, A. Askin, Y.S. Rammah, Comprehensive study on the structural, optical, physical and gamma photon shielding features of $B_2O_3–Bi_2O_3–PbO–TiO_2$ glasses using WinXCOM and Geant4 code. J. Mol. Struct. **1197**, 656–665 (2019)
22. M.S. Al-Buriahi, H. Arslan, B.T. Tonguç, Mass attenuation coefficients, water and tissue equivalence properties of some tissues by Geant4, XCOM and experimental data. Indian J. Pure Appl. Phys. (IJPAP) **57**(6), 433–437 (2019)
23. M.I. Sayyed, Y.S. Rammah, A.S. Abouhaswa, H.O. Tekin, B.O. Elbashir, $ZnO–B_2O_3–PbO$ glasses: synthesis and radiation shielding characterization. Phys. B **548**, 20–26 (2018)
24. A. Khanna, A. Saini, B. Chen, F. Gonzalez, B. Ortiz, Structural characterization of $PbO–B_2O_3–SiO_2$ glasses. Phys. Chem. Glasses Eur. J. Glass Sci. Technol. Part B **55**(2), 65–73 (2014)
25. R. Nowotny, *XMuDat: Photon Attenuation Data on PC* (IAEA-NDS-195, Vienna, 1998)
26. M.J. Berger, J.H. Hubbell, *XCOM: Photon Cross Sections Database*. National Institute of Stan and Technology, Gaithersburg, MD 20899, USA, 1987–1999. Web version 1.2. http://physics.nist.gov/xcom **(Originally published as NBSIR 87–3597 "XCOM: Photon Cross Section on a Personal Computer")**
27. L. Gerward, N. Guilbert, K.B. Jensen, H. Lerving, WinXCom—a program for calculating X-ray attenuation coefficients. Radiat. Phys. Chem. **74**, 653–654 (2004)
28. F. Akman, M.R. Kacal, M.I. Sayyed, H.A. Karataş, Study of gamma radiation attenuation properties of some selected ternary alloys. J. Alloys Compd. **782**, 315–322 (2019)
29. M.I. Sayyed, F. Akman, I.H. Gecibesler, H.O. Tekin, Measurement of mass attenuation coefficients, effective atomic numbers,

and electron densities for different parts of medicinal aromatic plants in low-energy region. Nucl. Sci. Tech. **29**, 144 (2018)
30. O. Agar, M.I. Sayyed, F. Akman, H.O. Tekin, M.R. Kacal, An extensive investigation on gamma ray shielding features of Pd/Ag-based alloys. Nucl. Eng. Technol. **51**, 853–859 (2019)
31. I. Bashter, Calculation of radiation attenuation coefficients for shielding concretes. Ann. Nucl. Energy **24**, 1389–1401 (1997)
32. I. Akkurt, R. Altindag, K. Gunoglu, H. Sarikaya, Photon attenuation coefficients of concrete including marble aggregates. Ann. Nucl. Energy **43**, 56 (2012)
33. http://www.schott.com/advanced_optics/english/products/optical-materials/special-materials/radiation-shielding-glasses/index.html
34. V.P. Singh, N.M. Badiger, J. Kaewkhao, Radiation shielding competence of silicate and borate heavy metal oxide glasses: comparative study. J. Non Cryst. Solids **404**, 167–173 (2014)
35. Y.S. Rammah, A.S. Abouhaswa, M.I. Sayyed, H.O. Tekin, R. El-Mallawany, Structural, UV and shielding properties of ZBPC glasses. J. Non Cryst. Solids **509**, 99–105 (2019)
36. R. El-Mallawany, M.I. Sayyed, M.G. Dong, Comparative shielding properties of some tellurite glasses: part 2. J. Non Cryst. Solids **474**, 16–23 (2017)
37. R. El-Mallawany, M.I. Sayyed, Comparative shielding properties of some tellurite glasses: part 1. Phys. B **539**, 133–140 (2018)